

Exact Diagonalization of $SU(N)$ Fermi-Hubbard Models

Thomas Botzung and Pierre Nataf 

*Laboratoire de Physique et Modélisation des Milieux Condensés, Université Grenoble Alpes and CNRS,
25 avenue des Martyrs, 38042 Grenoble, France*

 (Received 15 September 2023; revised 8 March 2024; accepted 14 March 2024; published 10 April 2024)

We show how to perform exact diagonalizations of $SU(N)$ Fermi-Hubbard models on L -site clusters separately in each irreducible representation (irrep) of $SU(N)$. Using the representation theory of the unitary group $U(L)$, we demonstrate that a convenient orthonormal basis, on which matrix elements of the Hamiltonian are very simple, is given by the set of *semistandard Young tableaux* (or, equivalently, the Gelfand-Tsetlin patterns) corresponding to the targeted irrep. As an application of this color factorization, we study the robustness of some $SU(N)$ phases predicted in the Heisenberg limit upon decreasing the on-site interaction U on various lattices of size $L \leq 12$ and for $2 \leq N \leq 6$. In particular, we show that a long-range color ordered phase emerges for intermediate U for $N = 4$ at filling $1/4$ on the triangular lattice.

DOI: [10.1103/PhysRevLett.132.153001](https://doi.org/10.1103/PhysRevLett.132.153001)

The Fermi-Hubbard model (FHM) is among the most important models in condensed matter [1–3]. In particular, the $SU(2)$ FHM on the square lattice might describe the physics of electrons carrying a spin one half in cuprate superconductors [3–5] and has motivated numerous theoretical investigations [6,7]. Considering N , the number of degenerate orbitals, as an integer parameter of the models, a natural extension of the $SU(N=2)$ FHM is the $SU(N)$ FHM [8–10].

This higher symmetry group Hamiltonian, first introduced as a theoretical tool to provide an asymptotic description of spins $1/2$ in the large N limit [11–14], can also describe some condensed matter systems like transition metal compounds [15,16] or graphene with $SU(4)$ spin valley symmetry or in twisted bilayer [17]. Alternatively, alkaline-earth cold atoms like ^{173}Yb or ^{87}Sr can simulate $SU(N)$ -invariant FHMs for N up to 10 on various engineered optical lattices [18–21]. Additionally, the continuous experimental achievements in this field [22–27] brought theoreticians to investigate these systems in order to look for exotic phases that would generalize their $N = 2$ counterpart.

Apart from some quantum Monte Carlo studies [28,29] addressing the $SU(N)$ FHM at half filling for a wide range of positive on-site interaction U , most of the theoretical investigations focused on the large U limit, where the atoms, in the Mott insulating phase, are described by $SU(N)$ Heisenberg models (HMs) [30–37]. Depending on the lattices and on the number of colors N , different two-dimensional phases are predicted at $T = 0$, among which the $SU(N)$ plaquette phases [38–42] are cousins of the valence bond states for spins $1/2$, the Néel long-range color ordered (LRO) states [34,35] are analogous to the famous (π, π) (respectively, 120°) Néel states existing on

the square [43,44] (respectively, the triangular [45,46]) lattice for $N = 2$, and diverse kinds of $SU(N)$ spin liquids [47–56] generalizing the Anderson resonating valence bond states [4,57]. Except for the one-dimensional system where there is a Bethe ansatz solution [58], the theoretical investigation of these models, based on advanced numerical tools, is challenging mainly because the dimension of the full Hilbert space on finite-size lattices increases exponentially, being equal to N^L , where L is the number of sites of the cluster, for filling $1/N$ (exactly one particle per site) in the $SU(N)$ HM.

However, it was realized that working in the $SU(N)$ singlet subspace, which usually contains the ground state (GS) in the antiferromagnetic case, is very advantageous as its dimension is much smaller than N^L . For instance, for $N = 6$ and $L = 12$, such a dimension is equal to 132, while $N^L \equiv 6^{12} \approx 2 \times 10^9$. In addition, the exact diagonalization (ED) of the HM directly in the $SU(N)$ singlet subspace can be made easy on the basis of standard Young tableaux (SYT) using the orthogonal representation of the group of permutations \mathcal{S}_L [59]. It is crucial to extend this theory to the $SU(N)$ FHM as the dimension of the full Hilbert space is even larger, i.e., equal to 2^{NL} . In fact, for $N = 6$, $L = 12$ at filling $1/6$ the dimension of the singlet subspace for the $SU(6)$ FHM is $\approx 14 \times 10^6$, while the full Hilbert space has dimension $2^{72} \approx 5 \times 10^{21}$.

In this Letter, we use the representation theory of the Lie group $U(L)$ to show how to perform ED of the $SU(N)$ FHM directly in each irreducible representation (irrep). After the description of the method, we apply the procedure to show some ED results on square and triangular clusters of size up to $L = 12$ and for N up to $N = 6$ to see how robust are some $SU(N)$ Mott insulating phases while decreasing the on-site repulsion.

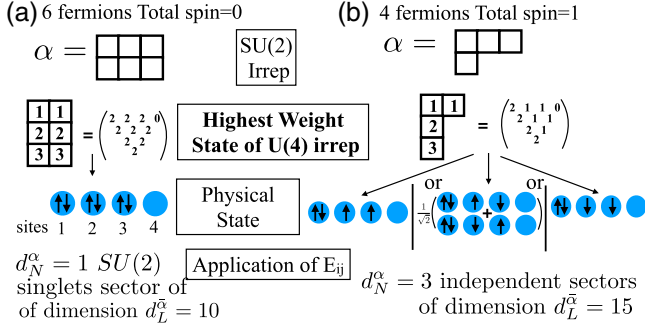


FIG. 1. Examples of $SU(N=2)$ irrep α for a $L=4$ -site cluster and $M=6$ fermions in (a) and $M=4$ fermions in (b). The Young tableaux are $\alpha = [3, 3]$ (respectively, $\alpha = [3, 1]$), representing singlets (respectively, spin 1) states. We associate the transpose YT, flipping the shape: $\alpha = [3, 3] \rightarrow \bar{\alpha} = [2, 2, 2]$ for (a) and $\alpha = [3, 1] \rightarrow \bar{\alpha} = [2, 1, 1]$ for (b). We fill up $\bar{\alpha}$ to get the highest weight state to which we associate d_N^{α} physical states, each of which generates an independent d_L^{α} -dimensional sector invariant under the application of the operators E_{ij} . See text for details.

The Hamiltonian for the $SU(N)$ FHM reads

$$H = \sum_{\langle i,j \rangle} (-t_{ij} E_{ij} + \text{H.c.}) + \frac{U}{2} \sum_{i=1}^L E_{ii}^2, \quad (1)$$

where the t_{ij} are the (possibly complex) hopping amplitude between sites i and j of a L -site finite cluster, and the on-site interaction amplitude is U . The $SU(N)$ -invariant hopping terms $E_{ij} = E_{ji}^{\dagger} = \sum_{\sigma=1}^N c_{i\sigma}^{\dagger} c_{j\sigma}$ satisfy the commutation relation of the $U(L)$ generators ($\forall 1 \leq i, j, k, l \leq L$),

$$[E_{ij}, E_{kl}] = \delta_{jk} E_{il} - \delta_{li} E_{kj}, \quad (2)$$

so that the Hamiltonian in Eq. (1), where the integer parameter N is *hidden*, can be seen as an element of the Lie algebra of the unitary group $U(L)$ [60]. It should be considered as the counterpart of the quantum permutation Hamiltonian for the $SU(N)$ -invariant HM, i.e., $H = \sum_{\langle i,j \rangle} J_{ij} P_{ij} + \text{H.c.}$, with P_{ij} (respectively, J_{ij}) the permutation (respectively, coupling constant) between interacting sites i and j , for which the representation theory of the algebra of the group of permutations was used to perform ED directly and separately in each irrep of $SU(N)$ [59,62].

We remind the reader that an irrep of $SU(N)$ is labeled by a Young tableau (YT) or shape α (see Fig. 1), the N rows of which represent N integers $\alpha = [\alpha_1, \alpha_2, \dots, \alpha_N]$ such that $\alpha_1 \geq \alpha_2 \geq \dots \geq \alpha_N \geq 0$ and $\sum_{i=1}^N \alpha_i = M$, where M is the number of particles [i.e., the filling is $M/(LN)$]. Calling $\mathcal{H}_L^{M,N}$, the Hilbert space for L sites and M $SU(N)$ fermions, its dimension $D_L^{M,N} \equiv \dim(\mathcal{H}_L^{M,N})$ is [63]

$$\sum_{\alpha} h_L^{\alpha} \prod_{i=1}^L \binom{N}{\bar{\alpha}_i} = \sum_{\alpha} d_N^{\alpha} d_L^{\alpha}, \quad (3)$$

where the sums on both sides run over all the YT α of M boxes, with maximum L columns and N rows. $\bar{\alpha} = [\bar{\alpha}_1, \dots, \bar{\alpha}_L]$ is defined as the *transpose* YT of α , transforming rows into columns (cf. Fig. 1 for some examples). On the lhs of Eq. (3), $\bar{\alpha}$ is a distribution of fermions: $\bar{\alpha}_j$ being the number of fermions (necessarily $\leq N$) on site j for $1 \leq j \leq L$; $\prod_{i=1}^L \binom{N}{\bar{\alpha}_i}$ is the number of states for such a distribution. The factor h_L^{α} , defined as $h_L^{\alpha} = L! / \prod_{k=0}^N (n_k^{\alpha})!$, where $n_k^{\alpha} = \text{Cardinal}\{j \in [1; L] : \bar{\alpha}_j = k\}$, is the number of distributions corresponding to a given partition $\bar{\alpha}$, while permuting the $\bar{\alpha}_j$ (or the site indices j) for $1 \leq j \leq L$. In the rhs of Eq. (3), d_N^{α} (respectively, d_L^{α}) stands for the dimension of the $SU(N)$ irrep α [respectively, the $U(L)$ irrep $\bar{\alpha}$] [71], which we can calculate using existing formulas [63]. These dimensions are equal to the number of semistandard Young tableaux (ssYT) of shape α (respectively, $\bar{\alpha}$) filled with numbers from 1 to N (respectively, L), since these latter form a basis of the $SU(N)$ or $U(L)$ irrep. Given a $U(L)$ irrep represented by some YT, a ssYT is filled up with integer numbers from 1 to L in nondescending order from left to right in any row (repetitions allowed), and in strictly ascending order (repetitions not allowed) from top to bottom in any column [cf. Fig. 1 and Eq. (4) for some examples].

As detailed below and in the Supplemental Material [63], for the color-invariant $SU(N)$ FHM [cf. Eq. (1)], the Hilbert space $\mathcal{H}_L^{M,N}$ can be decomposed, or *color-factorized*, following the rhs of the equation for the dimension $D_L^{M,N}$, i.e., Eq. (3). In particular, targeting a given collective $SU(N)$ irrep α , we will need to diagonalize a matrix of dimension d_L^{α} , and there will be d_N^{α} independent copies (some multiplicity) of the corresponding spectrum in the full energy spectrum of the model. For instance, when M is a multiple of N , one important sector is the $SU(N)$ singlet sector, as it usually contains the lowest energy eigenstates (in the large $U > 0$ limit, for instance); it is labeled by the perfectly rectangular N -row YT $\alpha = \alpha_{S,M} \equiv [M/N, M/N, \dots, M/N]$. In this case, $d_N^{\alpha_{S,M}} = 1$ and for $L=12$ at filling $1/N$ ($M=L$), one has, for instance, $d_{L=12}^{\alpha_{S,M=L}} = 13\,026\,013$ for $N=4$ and $d_{L=12}^{\alpha_{S,M=L}} = 14\,158\,144$ for $N=6$. This should be compared to the dimensions of the sector usually addressed in standard ED with a fixed number of fermions of each color [conserving the $U(1)$ symmetry], which is $d_{L,M,N}^{U(1)} = \binom{L}{M/N}^N$: one has $d_{L=M=12,N=4}^{U(1)} \approx 2.34 \times 10^9$ (respectively, $d_{L=M=12,N=6}^{U(1)} \approx 8.27 \times 10^{10}$). As N increases, it is more and more advantageous to implement the full $SU(N)$ symmetry, working in the $SU(N)$ singlet sector and, more generally, in a sector of a given irrep α .

For a given $U(L)$ irrep $\bar{\alpha}$, the *highest weight state* (*hw*s), uniquely (up to some similarity) and fully determines the irrep, as one can generate the entire basis by applications of the generators E_{ij} (for $1 \leq i, j \leq L$). The *hw*s is represented by the shape $\bar{\alpha}$ filled with 1 for the first row (of length $\bar{\alpha}_1$), 2 for the second row (of length $\bar{\alpha}_2$), etc.

(cf. Fig. 1). It is defined by the following properties: $E_{ij}|\text{hws}\rangle = \bar{\alpha}_i|\text{hws}\rangle \forall i \in \llbracket 1; L \rrbracket$ and $E_{ij}|\text{hws}\rangle = 0$ for $i < j$ [72]. Crucially, in $\mathcal{H}_L^{M,N}$, there are d_N^α orthonormal states $|\phi_{\alpha,k}^{\text{hws}}\rangle$ ($k = 1, \dots, d_N^\alpha$) that have these properties and can then be represented by the same ssYT associated with the $|\text{hws}\rangle$. For example, for the $SU(N)$ singlet irrep $\alpha_{S,M}$, there is only one state $|\phi_{\alpha,1}^{\text{hws}}\rangle$ and it is the product of $SU(N)$ singlets for sites $1, 2, \dots, M/N$, with no particles on sites $M/N + 1, \dots, L$ [cf. Fig. 1 and the Supplemental Material [63] for details about $SU(N)$ singlets].

On the basis of the ssYT, which are equivalent to the Gelfand-Tsetlin (GT) patterns [63,73], the matrix elements of the infinitesimal generators E_{pp} , which are the occupation numbers on site p for $p = 1, \dots, L$ and of E_{p-1p} (respectively, E_{pp-1}), which generalize the lowering operator J_- (respectively, J_+) for $U(2)$, are very simple. Found by Gelfand and Tsetlin [74], we detail them in the Appendix. As an illustrative example, for the $SU(4)$ adjoint irrep at filling $1/4$ for $L = 12$ (the basis has then 57972915 elements), we have, for instance,

$$E_{23} \begin{array}{|c|c|c|c|} \hline 1 & 1 & 2 & 3 \\ \hline 2 & 3 & 3 & 4 \\ \hline 4 & 5 & 6 & \\ \hline 5 & & & \\ \hline \end{array} = \sqrt{\frac{5}{6}} \begin{array}{|c|c|c|c|} \hline 1 & 1 & 2 & 2 \\ \hline 2 & 3 & 3 & 4 \\ \hline 4 & 5 & 6 & \\ \hline 5 & & & \\ \hline \end{array} + \sqrt{\frac{16}{6}} \begin{array}{|c|c|c|c|} \hline 1 & 1 & 2 & 3 \\ \hline 2 & 2 & 3 & 4 \\ \hline 4 & 5 & 6 & \\ \hline 5 & & & \\ \hline \end{array}. \quad (4)$$

Finally, from the successive applications of the commutation relations [Eq. (2)] and from $E_{ij} = E_{ji}^\dagger$, one gets the matrix representing the $SU(N)$ FHM Hamiltonian H [cf. Eq. (1)] in the irrep $\bar{\alpha}$, which corresponds to the $SU(N)$ irrep α .

We have applied this theory to study the FHM of Eq. (1) for uniform nearest neighbors hopping $t_{ij} \equiv t = 1$ as a function of U at filling $1/N$, starting from the Heisenberg limit ($U \rightarrow \infty$) and diminishing U . The ground states of the $SU(3)$ HM on the triangular lattice (TL) and of the $SU(5)$ HM on the square lattice (SL) are both Néel LRO states, with a three-sublattice ordering pattern for $SU(3)$ [35,75,76] and a (chess) knight move pattern for $SU(5)$ [59]. We give evidence of such orders by calculating the simple correlation patterns of the exact ground states of the FHM in Fig. 2 for $U = 10$. Moreover, the energy spectra plotted as a function of the quadratic Casimir C_2 [63,72] of the different irreps α exhibit an Anderson tower of states (Atos), which reveals the continuous symmetry breaking of $SU(3)$ [respectively, $SU(5)$] as shown in Fig. 3 (respectively, in the Supplemental Material [63]). We have checked the convergence in the limit $U \rightarrow \infty$ within each irrep α of the eigenenergies toward those of the HMs with the factor $2/U$. In fact, the group theory coefficients used in the protocol for the $SU(N)$ FHM converge [63] toward the ones needed in the algorithm for the $SU(N)$ HM [59].

While diminishing U , the structure of the energy spectra stays the same up to $U \sim 2.5$ (respectively, $U \sim 1$) for $SU(3)$ on the $L = 12$ TL [respectively, $SU(5)$ on the

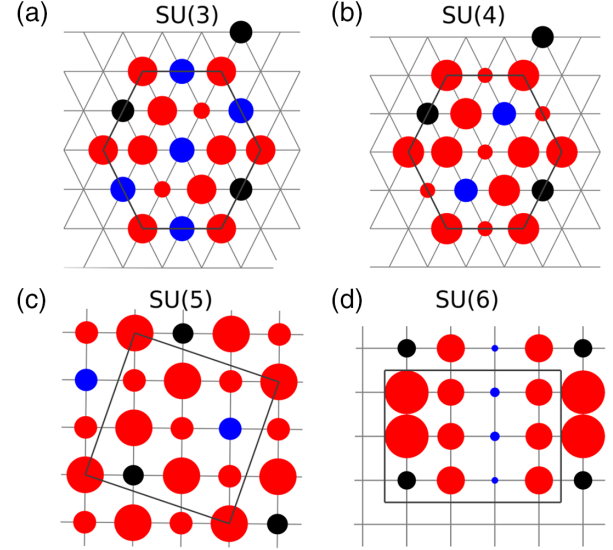


FIG. 2. Correlation patterns of the ground states of the FHM at filling $1/N$ for $U = 10$ in (a),(c),(d) and for $U = 12$ in (b). They are defined as $\langle P_{1j} \rangle - 1/N$, where $P_{1j} \equiv -1 + E_{1j}E_{j1}$, with the reference site 1 in black, and j the site indices being blue (red) for positive (negative) correlation, with area proportional to its absolute value. At the top, triangular lattice with $L = 12$ sites, for $SU(3)$ (a) compatible with the three-sublattice Néel order [35,75,76] and for $SU(4)$ (b) compatible with the four-sublattice Néel order [32]. (c) $SU(5)$ on the cluster $\sqrt{10} \times \sqrt{10}$, pattern compatible with the (chess) knight move LRO [59]; (d) $SU(6)$ on the 3×4 cluster, compatible with the $SU(6)$ plaquette state [42].

$L = 10$ SL]. Then, some energy plateau as a function of C_2 appears for smaller U , which is also true for $SU(2)$ on the TL, as shown in Fig. 3. Such a system should be in the metallic phase for $U \lesssim 8.5$, as expected from density-matrix renormalization group (DMRG) simulations on large cylinders [77], so that the plateau could be a signature of the metallic phase in the weak coupling limit. To further characterize the metallic phase and to locate its boundary, we show in Fig. 4 and in the Supplemental Material [63] the charge gap defined by $\Delta_c = E_0(M = L + 1) + E_0(M = L - 1) - 2E_0(M = L)$, where $E_0(M)$ is the minimal energy for the lattice with M fermions, which implies the diagonalization over all the relevant $M = L, L \pm 1$ box irreps $\bar{\alpha}$. It suggests that the metallic phase develops for $U \leq U_c = 9.8(\pm 0.4)$ for $SU(3)$ on a TL and for $U \leq U_c = 8.75(\pm 0.15)$ for $SU(5)$ on a SL, with apparently no intermediate phase between the latter and the LRO in the large U limit. The scenario of successive LRO phases, with different antiferromagnetic orders, like what was numerically observed in the $SU(3)$ FHM on the SL [78], does not seem to occur here, since the correlation patterns are monotonic [63]. However, the sizes of the clusters within reach of our ED method do not exclude such a scenario in the bulk limit.

The presence of an in-between phase, detectable on finite-size clusters, might occur when the HM limit is not a

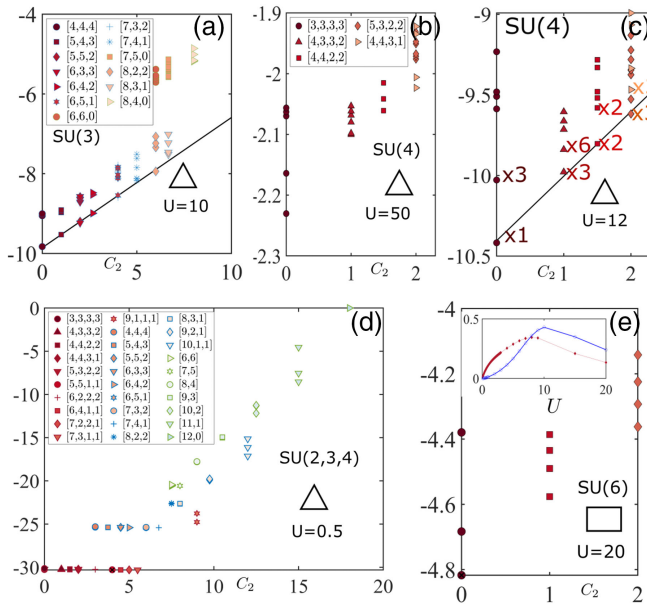


FIG. 3. Energy spectra of the FHM in Eq. (1) (with $t_{ij} \equiv 1$ at filling $1/N$) as a function of the quadratic Casimir C_2 for various values of U and N for the $L = 12$ periodic triangular lattice [(a)–(d)] and for the $L = 4 \times 3$ periodic square lattice in (e), where we focused on $N = 6$. Note that the constant $LU/2$ has been withdrawn. (c) The Atos is reminiscent of the one revealing the four-sublattice order in the HM with nnn couplings [32]. Inset of (e): spin (singlet) gap in blue (red).

LRO, such as for SU(3) on the honeycomb lattice [79]. The SU(4) FHM on the TL might enter into this category as the HM limit is a gapless quantum spin liquid [32,54,56]. In fact, while there are four low-lying energy SU(4) singlet states for $U = 50$ on the $L = 12$ site TL, when decreasing the interaction, the singlet gap (defined as the gap within the singlet irrep $\alpha_{S,M}$) starts increasing and an emerging Atos appears for $U \lesssim 15$ (cf. Fig. 3 with both $U = 12$ and $U = 50$), which is similar to the one occurring in a pseudo-HM with next-nearest neighbor (nnn) couplings on the same $L = 12$ TL cluster [32]. The nnn couplings, which are present at order 4 in t/U in the large U limit [53], were shown to stabilize a four-sublattice order [32], also apparent in the correlation patterns of our Fig. 2. From the charge gap shown in Fig. 4, the boundary between this phase and the metallic phase occurs around $U = U_c = 11.2 \pm 0.2$. Like for the other systems, such a value slightly changes for larger L due to finite-size effects, as illustrated for SU(2), $L = 12$, and $L = 16$ in the Supplemental Material [63]. We also show, in Fig. 4(b), the SU(N) spin gaps Δ_s defined as the difference between the minimal energy of the SU(N) adjoint irrep sector (corresponding to $\alpha = [M/N + 1, M/N, \dots, M/N - 1]$) and that of the singlet sector (i.e., for $\alpha = \alpha_{S,M}$). The spin gaps Δ_s , which are also impacted by finite-size effects [63], exhibit some peaks at values of U that roughly match with the values U_c for each N .

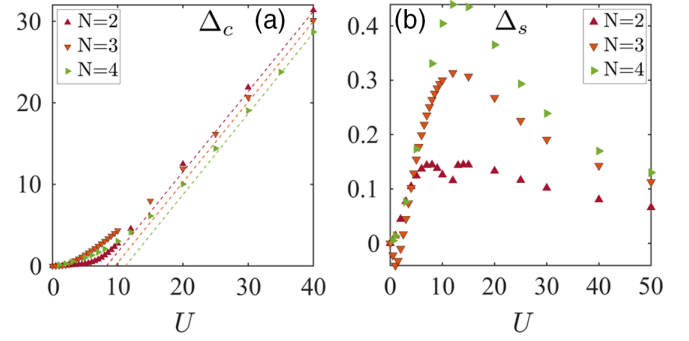


FIG. 4. (a) Charge gaps Δ_c for the FHM on the $L = 12$ sites triangular lattice for $N = 2, 3$, and 4 at filling $1/N$. The dashed lines (cf. the Supplemental Material [63] for the fitting procedure) cross the x axis at $U \simeq 8.6$ for $N = 2$, $U \simeq 9.8$ for $N = 3$, and $U \simeq 11.2$ for $N = 4$ separating the small U metallic phase from the Mott insulators. (b) SU(N) spin gaps Δ_s .

Finally, we have investigated the SU(6) FHM on the SL, as the HM limit is also not a LRO but a plaquette state [42]. Through the correlation pattern of the GS on a 4×3 periodic SL for $U = 10$ in Fig. 2, we found some evidence of the six-site plaquette state in the Mott phase, a feature confirmed by the presence of two low-lying energy SU(6) singlet states, compatible with the periodic boundary conditions, for large U (i.e., $U = 20$, cf. Fig. 3). When U decreases, the spin gap becomes smaller than the singlet gap, suggesting a change of phases. However, with the current version of our code and with the limitation of our computational resources, the necessary calculation of the charge gap was too demanding, leaving open both the question of the size of the metallic phase and the presence of some intermediate phase.

To conclude, we found an efficient protocol to perform ED of the FHM on L -site clusters directly in each SU(N) irrep, which uses the set of ssYT (or GT patterns) as a convenient basis with matrix elements of the $U(L)$ group generators. This approach, which generalizes the use of SYT for SU(N) in HMs [59], dramatically reduces the dimension of the matrices to diagonalize. We applied our method to study the survival of the SU(N) Mott phases from $N = 3$ to $N = 6$ on TL and SL when the on-site interaction U decreases. In particular, we found an emerging intermediate LRO phase for SU(4) on the TL, reminiscent of the four-sublattice order in the HM with nnn couplings [32].

Among the perspectives, since the SU(N) FHM can be seen as a fine-tuned version of the Sp(N) FHM [80], one could generalize our approach to Hamiltonians invariant under Sp(N) [19,81,82]. It would be numerically helpful, as the dimension of the Sp(N) singlet sector is also much smaller than that of the sector used in traditional ED [63]. However, GT-type bases for finite-dimensional irreps of

$\text{Sp}(N)$ are more complicated to handle than those for the irreps of $\text{SU}(N)$ [83,84]. Other perspectives would be the implementation of the ssYT basis in tensor networks and DMRG algorithms, in a fashion similar to what was done with the SYT for the HM [85,86], and the combination of both the implementation of the $\text{SU}(N)$ and of the spatial symmetries in ED.

We acknowledge F. Mila for fruitful discussions and S. Gozel for a critical reading of the manuscript, as well as A. Laeuchli and C. Ganahl who gave us some 15 digit $\text{SU}(3)$ FHM eigenenergies [53] for data comparisons. This work has been supported by an Emergence grant from CNRS Physique.

Appendix.—The matrix elements of the infinitesimal generators between equal or consecutive sites E_{pp} , E_{p-1p} , E_{pp-1} , take a simple form on the basis of the ssYT. Calling $|\nu\rangle$ a ssYT, one has for $p = 1, \dots, L$,

$$E_{pp}|\nu\rangle = \text{Cardinal}\{p \in \nu\}|\nu\rangle, \quad (\text{A1})$$

where $\text{Cardinal}\{p \in \nu\}$ is equal to the number of occurrences of p inside $|\nu\rangle$, corresponding to the occupation number on site p (cf. Fig. 1 for some examples).

Second, calling $|\nu\rangle$ a ssYT, one has for $p = 2, \dots, L$,

$$E_{p-1p}|\nu\rangle = \sum_{j=1}^{p-1} a_{p-1}^j F_{p-1}^j |\nu\rangle, \quad (\text{A2})$$

where the tableau operators F_{p-1}^j transform the number p in the j th row in $|\nu\rangle$ into $p-1$. As for the coefficients a_{p-1}^j , which vanish in the case where such a transformation is not possible, either because there is no p in the j th row of $|\nu\rangle$ or because the resulting tableau is not a proper ssYT, they read [63,87]

$$a_{p-1}^j = \left| \frac{\prod_{i=1}^p (l_{i,p} - l_{j,p-1}) \prod_{i=1}^{p-2} (l_{i,p-2} - l_{j,p-1} - 1)}{\prod_{i \neq j} (l_{i,p-1} - l_{j,p-1}) \prod_{i \neq j} (l_{i,p-1} - l_{j,p-1} - 1)} \right|^{1/2}, \quad (\text{A3})$$

where $l_{k,q} = m_{k,q} - k$ with $m_{k,q}$ as the length of the k th row of the subtableau that remains when we delete all the boxes containing numbers $> q$ in $|\nu\rangle$. Finally, from $E_{ij} = E_{ji}^\dagger$, we obtain the matrix elements of E_{pp-1} for $p = 2, \dots, L$.

- [5] F. C. Zhang and T. M. Rice, *Phys. Rev. B* **37**, 3759 (1988).
- [6] D. P. Arovas, E. Berg, S. A. Kivelson, and S. Raghu, *Annu. Rev. Condens. Matter Phys.* **13**, 239 (2022).
- [7] M. Qin, T. Schäfer, S. Andergassen, P. Corboz, and E. Gull, *Annu. Rev. Condens. Matter Phys.* **13**, 275 (2022).
- [8] R. Assaraf, P. Azaria, M. Caffarel, and P. Lecheminant, *Phys. Rev. B* **60**, 2299 (1999).
- [9] C. Honerkamp and W. Hofstetter, *Phys. Rev. Lett.* **92**, 170403 (2004).
- [10] S. Capponi, P. Lecheminant, and K. Totsuka, *Ann. Phys. (Amsterdam)* **367**, 50 (2016).
- [11] I. Affleck, *Nucl. Phys.* **B265**, 409 (1986).
- [12] I. Affleck and J. B. Marston, *Phys. Rev. B* **37**, 3774 (1988).
- [13] D. S. Rokhsar, *Phys. Rev. B* **42**, 2526 (1990).
- [14] M. Marder, N. Papanicolaou, and G. C. Psaltakis, *Phys. Rev. B* **41**, 6920 (1990).
- [15] S. K. Pati, R. R. P. Singh, and D. I. Khomskii, *Phys. Rev. Lett.* **81**, 5406 (1998).
- [16] M. G. Yamada, M. Oshikawa, and G. Jackeli, *Phys. Rev. Lett.* **121**, 097201 (2018).
- [17] Y.-H. Zhang, D. N. Sheng, and A. Vishwanath, *Phys. Rev. Lett.* **127**, 247701 (2021).
- [18] C. Wu, J. P. Hu, and S.-c. Zhang, *Phys. Rev. Lett.* **91**, 186402 (2003).
- [19] C. Wu, *Mod. Phys. Lett. B* **20**, 1707 (2006).
- [20] A. V. Gorshkov, M. Hermele, V. Gurarie, C. Xu, P. S. Julienne, J. Ye, P. Zoller, E. Demler, M. D. Lukin, and A. Rey, *Nat. Phys.* **6**, 289 (2010).
- [21] M. A. Cazalilla and A. M. Rey, *Rep. Prog. Phys.* **77**, 124401 (2014).
- [22] S. Taie, R. Yamazaki, S. Sugawa, and Y. Takahashi, *Nat. Phys.* **8**, 825 (2012).
- [23] C. Hofrichter, L. Riegger, F. Scazza, M. Höfer, D. R. Fernandes, I. Bloch, and S. Fölling, *Phys. Rev. X* **6**, 021030 (2016).
- [24] B. Abeln, K. Sponselee, M. Diem, N. Pintul, K. Sengstock, and C. Becker, *Phys. Rev. A* **103**, 033315 (2021).
- [25] S. Taie, E. Ibarra-García-Padilla, N. Nishizawa, Y. Takasu, Y. Kuno, H.-T. Wei, R. T. Scalettar, K. R. A. Hazzard, and Y. Takahashi, *Nat. Phys.* **18**, 1356 (2022).
- [26] D. Tusi, L. Franchi, L. F. Livì, K. Baumann, D. Benedicto Orenes, L. Del Re, R. E. Barfknecht, T. W. Zhou, M. Inguscio, G. Cappellini, M. Capone, J. Catani, and L. Fallani, *Nat. Phys.* **18**, 1201 (2022).
- [27] G. Pasqualetti, O. Bettermann, N. D. Oppong, E. Ibarra-García-Padilla, S. Dasgupta, R. T. Scalettar, K. R. A. Hazzard, I. Bloch, and S. Fölling, *Phys. Rev. Lett.* **132**, 083401 (2024).
- [28] D. Wang, Y. Li, Z. Cai, Z. Zhou, Y. Wang, and C. Wu, *Phys. Rev. Lett.* **112**, 156403 (2014).
- [29] S. Xu, J. T. Barreiro, Y. Wang, and C. Wu, *Phys. Rev. Lett.* **121**, 167205 (2018).
- [30] N. Read and S. Sachdev, *Nucl. Phys.* **B316**, 609 (1989).
- [31] Y. Q. Li, M. Ma, D. N. Shi, and F. C. Zhang, *Phys. Rev. Lett.* **81**, 3527 (1998).
- [32] K. Penc, M. Mambrini, P. Fazekas, and F. Mila, *Phys. Rev. B* **68**, 012408 (2003).
- [33] M. Greiter and S. Rachel, *Phys. Rev. B* **75**, 184441 (2007).

-
- [1] J. Hubbard, *Proc. R. Soc. A* **276**, 238 (1963).
 - [2] M. C. Gutzwiller, *Phys. Rev. Lett.* **10**, 159 (1963).
 - [3] D. J. Scalapino, *Rev. Mod. Phys.* **84**, 1383 (2012).
 - [4] P. W. Anderson, *Science* **235**, 1196 (1987).

- [34] P. Corboz, A. M. Läuchli, K. Penc, M. Troyer, and F. Mila, *Phys. Rev. Lett.* **107**, 215301 (2011).
- [35] B. Bauer, P. Corboz, A. M. Läuchli, L. Messio, K. Penc, M. Troyer, and F. Mila, *Phys. Rev. B* **85**, 125116 (2012).
- [36] R. Bondesan and T. Quella, *Nucl. Phys.* **B886**, 483 (2014).
- [37] A. Weichselbaum, S. Capponi, P. Lecheminant, A. M. Tsvelik, and A. M. Läuchli, *Phys. Rev. B* **98**, 085104 (2018).
- [38] A. Paramekanti and J. B. Marston, *J. Phys. Condens. Matter* **19**, 125215 (2007).
- [39] P. Corboz, K. Penc, F. Mila, and A. M. Läuchli, *Phys. Rev. B* **86**, 041106(R) (2012).
- [40] T. C. Lang, Z. Y. Meng, A. Muramatsu, S. Wessel, and F. F. Assaad, *Phys. Rev. Lett.* **111**, 066401 (2013).
- [41] P. Nataf, M. Lajkó, P. Corboz, A. M. Läuchli, K. Penc, and F. Mila, *Phys. Rev. B* **93**, 201113(R) (2016).
- [42] O. Gauthé, S. Capponi, M. Mambrini, and D. Poilblanc, *Phys. Rev. B* **101**, 205144 (2020).
- [43] P. W. Anderson, *Phys. Rev.* **86**, 694 (1952).
- [44] E. Manousakis, *Rev. Mod. Phys.* **63**, 1 (1991).
- [45] B. Bernu, P. Lecheminant, C. Lhuillier, and L. Pierre, *Phys. Rev. B* **50**, 10048 (1994).
- [46] L. Capriotti, A. E. Trumper, and S. Sorella, *Phys. Rev. Lett.* **82**, 3899 (1999).
- [47] F. Wang and A. Vishwanath, *Phys. Rev. B* **80**, 064413 (2009).
- [48] M. Hermele and V. Gurarie, *Phys. Rev. B* **84**, 174441 (2011).
- [49] P. Corboz, M. Lajkó, A. M. Läuchli, K. Penc, and F. Mila, *Phys. Rev. X* **2**, 041013 (2012).
- [50] H.-H. Lai, *Phys. Rev. B* **87**, 205131 (2013).
- [51] G. Chen, K. R. A. Hazzard, A. M. Rey, and M. Hermele, *Phys. Rev. A* **93**, 061601(R) (2016).
- [52] P. Nataf, M. Lajkó, A. Wietek, K. Penc, F. Mila, and A. M. Läuchli, *Phys. Rev. Lett.* **117**, 167202 (2016).
- [53] C. Boos, C. J. Ganahl, M. Lajkó, P. Nataf, A. M. Läuchli, K. Penc, K. P. Schmidt, and F. Mila, *Phys. Rev. Res.* **2**, 023098 (2020).
- [54] A. Keselman, B. Bauer, C. Xu, and C.-M. Jian, *Phys. Rev. Lett.* **125**, 117202 (2020).
- [55] J.-Y. Chen, J.-W. Li, P. Nataf, S. Capponi, M. Mambrini, K. Totsuka, H.-H. Tu, A. Weichselbaum, J. von Delft, and D. Poilblanc, *Phys. Rev. B* **104**, 235104 (2021).
- [56] H.-K. Jin, R.-Y. Sun, H.-H. Tu, and Y. Zhou, *Sci. Bull.* **67**, 918 (2022).
- [57] P. W. Anderson, *Mater. Res. Bull.* **8**, 153 (1973).
- [58] B. Sutherland, *Phys. Rev. B* **12**, 3795 (1975).
- [59] P. Nataf and F. Mila, *Phys. Rev. Lett.* **113**, 127204 (2014).
- [60] Or, more precisely, of its universal enveloping algebra [61], since it contains some square of generators.
- [61] J. Dixmier, *Enveloping Algebras*, North-Holland Mathematical Library (North-Holland Publishing Company, Amsterdam, 1977).
- [62] K. Wan, P. Nataf, and F. Mila, *Phys. Rev. B* **96**, 115159 (2017).
- [63] See Supplemental Material at <http://link.aps.org/supplemental/10.1103/PhysRevLett.132.153001> for some details about representation theory and for some complementary numerical results, which includes Refs. [64–70].
- [64] H. Weyl, *Math. Z.* **23**, 271 (1925).
- [65] G. de B. Robinson, *Representation Theory of the Symmetric Group* (Edinburgh University Press, Edinburgh, 1961).
- [66] M. Hamermesh, *Group Theory and Its Application to Physical Problems*, Corr. ed. (Dover, New York, NY, 1989).
- [67] J.-Q. Chen, J. Ping, and F. Wang, *Group Representation Theory for Physicists* (World Scientific Publishing Company, Singapore, 2002).
- [68] A. Young, *Proc. London Math. Soc.* **s1-33**, 97 (1900).
- [69] K. Pilch and A. N. Schellekens, *J. Math. Phys. (N.Y.)* **25**, 3455 (1984).
- [70] R. Cahn, *Semi-Simple Lie Algebras and Their Representations* (Dover Publications, New York, 2014).
- [71] The irreps of $U(N)$ or $SU(N)$ are basically the same [63]; distinction is relevant when we include or exclude representation of generators with nonvanishing trace, such as some combinations of E_{ii} .
- [72] J. Paldus, *J. Math. Chem.* **59**, 1 (2021).
- [73] A. Alex, M. Kalus, A. Huckleberry, and J. von Delft, *J. Math. Phys. (N.Y.)* **52**, 023507 (2011).
- [74] I. M. Gelfand and M. L. Tsetlin, *Dokl. Akad. Nauk SSSR* **71**, 825 (1950).
- [75] H. Tsunetsugu and M. Arikawa, *J. Phys. Soc. Jpn.* **75**, 083701 (2006).
- [76] A. Läuchli, F. Mila, and K. Penc, *Phys. Rev. Lett.* **97**, 087205 (2006).
- [77] A. Szasz, J. Motruk, M. P. Zaletel, and J. E. Moore, *Phys. Rev. X* **10**, 021042 (2020).
- [78] C. Feng, E. Ibarra-García-Padilla, K. R. A. Hazzard, R. Scalettar, S. Zhang, and E. Vitali, *Phys. Rev. Res.* **5**, 043267 (2023).
- [79] S. S. Chung and P. Corboz, *Phys. Rev. B* **100**, 035134 (2019).
- [80] C. Wu and S.-C. Zhang, *Phys. Rev. B* **71**, 155115 (2005).
- [81] R. Flint, M. Dzero, and P. Coleman, *Nat. Phys.* **4**, 643 (2008).
- [82] A. Ramires, *Phys. Rev. A* **96**, 043604 (2017).
- [83] A. I. Molev, *Commun. Math. Phys.* **201**, 591 (1999).
- [84] A. I. Molev, arXiv:math/0211289.
- [85] P. Nataf and F. Mila, *Phys. Rev. B* **97**, 134420 (2018).
- [86] S. Gozel, P. Nataf, and F. Mila, *Phys. Rev. Lett.* **125**, 057202 (2020).
- [87] N. J. Vilenkin and A. U. Klimyk, *Representation of Lie Groups and Special Functions* (Kluwer Academic Publishers, Dordrecht, 1992), Vol. 3.